Korean J. Chem. Eng., 36(10), 1708-1715 (2019)
DOI: 10.1007/s11814-019-0360-5

pISSN: 0256-1115
eISSN: 1975-7220

Synthesis of bi-functionalized ionic liquid - mesoporous alumina composite material and its CO_2 capture capacity

Liwei Sun* **and Shaokun Tang*,**,†**

*Key Laboratory for Green Chemical Technology of Ministry of Education, School of Chemical Engineering & Technology, Tianjin University, Tianjin 300350, China
**Collaborative Innovation Center of Chemical Science and Engineering (Tianjin), Tianjin University, Tianjin 300072, China
(*Received 9 April 2019 • accepted 9 August 2019*)

Abstract−Bi-functionalized ionic liquid (IL) - mesoporous alumina (MA) composite material was synthesized and used for CO_2 capture. Ordered mesoporous alumina was synthesized by self-assembly method with aluminum isopropoxide as aluminum source. Then bi-functionalized ionic liquid 1-methoxyethyl-3-methyl imidazole glycinate ([MOEmim][Gly]) was immobilized on mesoporous alumina by ultrasonic-assisted impregnation method. Ordered mesostructure of alumina keeps well in the composite material. Compared with bi-functionalized ionic liquid, thermal stability of the composite material greatly improved. Finally, CO_2 capture capacity of IL-MA composite material was studied under different temperatures. On the basis of both capture capacity and capture rate, 40 °C is the optimal temperature. The capture capacity is 1.42 mol·mol IL^{-1} - equivalent to 144 mg·g $sorbent^{-1}$, which is higher than IL or MA alone. Furthermore, the capture capacity of composite material almost maintains constant after eight capture-regeneration cycles.

Keywords: Ionic Liquid, Mesoporous Alumina, Immobilization, Impregnation, Carbon Dioxide Capture

INTRODUCTION

The emission control of carbon dioxide (CO_2) into the atmosphere has attracted signification attention as a result of massive fossil fuel combustion. As a main greenhouse gas, CO_2 has more than 50 years life-time in the atmosphere and can lead to various environmental problems such as rising sea levels, higher ocean acidity and the melting of glaciers [1,2], which threaten human existence. Various techniques such as absorption [3,4], adsorption [1,5], membrane separation [2,6] have been developed for CO_2 capture. One of the most commercially utilized methods is chemical absorption by conventional amine solutions. These solutions possess acceptable absorption capacity, but they also have several drawbacks, including high energy penalty, solvent loss, equipment corrosion and extra installation cost, restricting their further development [3].

Ionic liquids (ILs) have negligible vapor pressure, high thermal stability as well as widely tunable properties [7]. They are regarded as substitutions of conventional organic solvents because of no production of VOCs in usage and regeneration process of ionic liquids. And they have been widely reported for CO_2 capture and separation by the aid of the functionalization of cation and/or anion [3,7,8]. It has been proved that amino-, ether-, and phenol-functionalized ILs were good CO_2 absorbents [9-11]. Bi-functionalized ILs, also named as dual functional ILs, refer to ionic liquids which contain two types of the same or different functional groups. Compared with conventional ILs or mono-functionalized ILs, bi-functionalized ILs can further improve CO_2 capture capacity on account of more functional groups having affinity with CO_2 [10]. In this paper, bi-functionalized ionic liquid 1-methoxyethyl-3-methylimidazolium glycinate ([MOEmim][Gly]) with ether group on the cation and amine group on the anion was selected and synthesized for highly efficient CO_2 capture based on high solubility and reactivity of the two groups to CO_2 as well as low cost of amino acid [3,10]. But high viscosity and low mass transfer rate of ionic liquids severely restrict their application in industrial areas [11]. To reduce the viscosity of reaction system and increase contact area between ILs and CO_2, supported ionic liquids (SILs) are introduced by impregnating [12,13] or grafting [14,15] methods. Because ionic liquids can be incorporated into the pores or dispersed on the surface of solid supports, the mass transfer resistance of CO_2 in sorbents can be decreased [13]. Several porous materials such as alumina [12], silica [13,14], molecular sieve [15] and activated carbon [16] are being studied as the supports of ionic liquids for CO_2 capture or separation.

Mesoporous materials possess highly uniform pore size, large pore volume and high specific surface area, and have been applied in the fields of adsorption-separation [12,13,16] and catalysts [17,18]. In recent years, mesoporous alumina (MA) has attracted considerable attention because of its large surface area and regular mesostructure. Compared to other solid supports, mesoporous alumina has high resistance to steam and good mechanical and thermal stability [19,20], which has been applied in a variety of fields such as catalysis [17], pollution treatment [21], gas adsorption [12,22,23] and so on. Ionic liquids supported on alumina materials for CO_2 capture or separation have been studied [11,12,19,20,24,25], which can increase the contact area of ionic liquid and CO_2. Wan et al. [12] selected tetrabutylphosphonium (P_{4444}) as cation and imidazole or 3-aminopyrazole as anion to prepare two kinds of basic ILs, and the ILs were immobilized on mesoporous alumina or silica for CO_2

†To whom correspondence should be addressed.
E-mail: shktang@tju.edu.cn

capture at elevated temperature. The highest adsorption capacity reached 81 mg·g^{-1} at 120 °C. Balsamo et al. [25] prepared mesoporous alumina-supported [Emim][Gly] ionic liquid at different loadings (5, 9 and 16% wt) by impregnation method and analyzed CO_2 adsorption on those materials. CO_2 adsorption capacity was 111 mg·g^{-1} IL for Al-[Emim][Gly] 16 at 30 °C. Although both IL functionalization and adsorbents support have been investigated, the CO_2 capture capacity of the composite material needs to be further improved.

Bi-functionalized ionic liquids for CO_2 capture have been studied in recent years [26,27]. To the best of our knowledge, there are few researches about bi-functionalized ionic liquids-modified adsorbents for CO_2 capture. In this study, bi-functionalized IL-MA composite materials were synthesized by ultrasonic-assisted impregnation method and CO_2 capture performance of IL-MA composite material was evaluated in the temperature range of 25-100 °C. Through the combination of physical adsorption and chemical absorption, CO_2 capture capacity of IL-MA composite material should be further enhanced as compared to pure ionic liquid or mesoporous alumina. CO_2 capture-regeneration cycle life of IL-MA composite material was also investigated.

EXPERIMENTAL

1. Materials

Aluminum isopropoxide, methanol (≥99.8%), citric acid (≥99.5%) were obtained from Guangfu Fine Chemical Industry Research Institute (Tianjin, China). Triblock copolymer F127 was received from Sigma Aldrich (Shanghai, China). Acetonitrile (≥99.9%) was purchased from Yuanli Chemical Co., Ltd (Tianjin, China). Acetone (≥99.5%), monoethanolamine (MEA, ≥99.0%), Hydrochloric acid (HCl, 36-38 wt%) and absolute ethanol (≥99.7%) were received from Jiangtian Chemical Technology Co., Ltd (Tianjin, China). Carbon dioxide (99.99%) was supplied from the steel cylinder was purchased from Tianjin Liufang Industrial Gases Co., Ltd. (China). All the chemicals were commercially available and used without further purification.

2. Synthesis of Bi-functionalized Ionic Liquid [MOEmim][Gly]

Bi-functionalized ionic liquid [MOEmim][Gly] was synthesized in our reported experiment [26] as shown in Scheme 1. First, 1-methylimidazole and 2-chloroethyl methyl ether was stirred and heated at 80 °C for 48 h under nitrogen atmosphere and reflux condition. Then, intermediate [MOEmim]Cl was obtained and anion-exchanged with $NaOCOCH_2NH_2$ at 40 °C for 36 h with acetone as solvent. Finally, [MOEmim][Gly] ionic liquid was purified *via* acetonitrile/methanol (V : V, 9 : 1) mixed solvent.

3. Synthesis of Ordered Mesoporous Alumina

The ordered mesoporous alumina was synthesized according to the literature [28,29] with quite a few modifications. First, the transparent alumina sol was prepared by dissolving F127, aluminum isopropoxide, citric acid and 36-38 wt% HCl in absolute ethanol with vigorous stirring at 40 °C for 5 h. Then the solvent was evaporated in DGG-9240BD electricity heat drum wind drying oven (Shanghai Senxin Experimental Instrument, China) at 60 °C for 48 h, where aluminum and F127 could form ordered mesophases. Finally, the highly ordered mesoporous structure was shaped with the F127 removal by calcinating at 700 °C for 4 h in SX2-2.5-10 muffle furnace (Tianjin Zhonghuan Electric, China).

4. Synthesis of IL-MA Composite Material

The bi-functionalized IL-MA composite material was prepared as follows. First, 20 mL of acetone and 2.0 g of [MOEmim][Gly] were mixed with 1.5 g of ordered mesoporous alumina in a 50-mL conical flasks at room temperature. Then, the mixture was ultrasonic impregnated for 60 min by KQ-200KDE ultrasonic cleaner (Kunshan Ultrasonic Instrument, China) and the mixed solution was filtered. Finally, residue was dried at 85 °C for 8-9 h in DH-204 electrothermal constant-temperature drying oven (Tianjin Zhonghuan Electric, China) and then IL-MA composite material was obtained.

5. Characterizations of Mesoporous Alumina and IL-MA Composite Material

The structures and physical properties of mesoporous alumina and IL-MA composite material were characterized using the following analytical instruments. The microstructure, morphologies and elemental analysis of samples were observed by JEM-2100 transmission electron microscopy (TEM, JEOL, Japan) and Nanosem 430 scanning electron microscopy (SEM, FEI, USA) equipped with an energy disperse spectroscope. Powder X-ray diffraction (XRD) patterns were recorded on a D/MAX-2500 X-ray diffractometer (Rigaku, Japan) in the 0.5-5° range and D8-Focus X-ray diffractometer (Bruker, Germany) with Cu Kα radiation (λ=1.5418 Å) in the range of 10-80°, respectively. VERTEX 70 Fourier transform infrared (FT-IR) spectrometer (Bruker, Germany) with KBr pellet was applied to examine the vibrational spectra of bi-functionalized ionic liquid, mesoporous alumina and IL-MA composite material. The masses of sample and KBr kept constant at 2 mg and 200 mg, respectively. The spectra were acquired in a wavenumber range between 400 and 4,000 cm^{-1}. Nitrogen adsorption-desorption isotherm was measured on an ASAP analyzer (Tristar 3000, Micromeritics, USA) at −196 °C. Thermal gravimetric (TG) analyses of [MOEmim][Gly] and IL-MA composite material were measured with TG 209 F3 Tarsus Thermo gravimetric Analyzer (Netzsch, Germany) heated from 40 to 800 °C with a temperature ramp of 10 °C/min in nitrogen atmosphere. And TG analysis also was used as an ancillary study of the ionic liquid loading capacity of IL-MA composite materials. The calculation formula is shown as follows:

$$\eta=(m_1-m_2)/m_1 \quad (1)$$

where η (gIL·gMA^{-1}) is the ionic liquid loading capacity of IL-MA composite material. m_1 (g) and m_2 (g) are the masses of IL-MA composite material at initial and complete decomposition of bi-

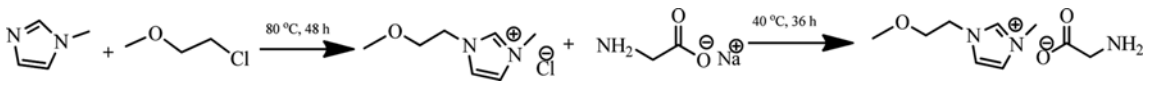

Scheme 1. Synthetic route of bi-functionalized ionic liquid [MOEmim][Gly].

functionalized ionic liquid, respectively.

6. Experimental Procedure for Carbon Dioxide Capture

In a typical CO_2 capture, the sorbent (IL, MA or IL-MA composite material) was placed in a 50-conical or U-shaped tube (Φ=7 mm) with rubber plug. Polytetrafluoroethylene (PTEF) membrane was also used to prevent the humid atmosphere from entering the system. Prior to measurement, the oil bath was heated at a desired temperature which was controlled by a digital thermometer system with a thermocouple within ±0.1 °C precision. The total inlet CO_2 flow rate was controlled at 100 mL/min by a mass flow controller (MFC, Beijing Seven-star Electronics, accuracy ±1%) through a 2 mm plastic soft tube. The outlet CO_2 flow rate was measured by a mass flow meter (MFM, Beijing Seven-star Electronics, accuracy ±1%). And the inlet and outlet volume of CO_2 were recorded at an interval of ten minutes. The equilibrium point for CO_2 capture was identified by the indication of the outlet flow rate equal to the inlet CO_2 flow rate. Here the capture capacity is the captured CO_2 mole quantity per mole ionic liquid based on the unit of mol·mol IL^{-1} or the captured CO_2 mass per gram adsorbent based on the unit of $mg \cdot g^{-1}$ at equilibrium stage. The capture curves of CO_2 into IL-MA composite material were measured under different temperatures (25-100 °C). And the capture curves of CO_2 into ionic liquid or mesoporous alumina alone were studied under the optimum capture conditions of IL-MA composite material. All tests were performed at ambient pressure and the adsorption time was 3 h. Each experiment was repeated at least three times to ensure reliability of data collected, and deviation of the date was no more than 2%.

Material regenerability is an important issue for gas capture and separation. So saturated IL-MA composite material was heated at 150 °C for 12 h to remove captured CO_2. The regenerated material was cycled to another CO_2 uptake experiment.

RESULTS AND DISCUSSION

1. Characterization of Ordered Mesoporous Alumina

The morphology and structure of mesoporous alumina can be observed by electron microscopy at micro level. TEM and SEM images of mesoporous alumina are shown in Fig. 1. The as-prepared sample presents regularly ordered channel and uniform pore size from TEM image (Fig. 1(a)). SEM image in Fig. 1(b) indicates that the obtained sample is irregular bulk. Uneven and porous external surface is visible in the higher magnification SEM image (Fig. 1(c)).

The nitrogen adsorption-desorption isotherm of the mesoporous alumina is shown in Fig. 2(a), which belongs to type IV curve with H1 type hysteresis loop. The result suggests that as-prepared alumina is ordered mesoporous material. And the sample possesses large specific surface area of 350 $m^2 \cdot g^{-1}$ and a total pore volume of 1.18 $cm^3 \cdot g^{-1}$. A narrow peak in the Barrett-Joyner-Halenda (BJH) pore-size distribution curve (shown in Fig. 2(b)) is centered at 5.38 nm, which is indicative of the uniform mesopores in this material [17].

The small-angle X-ray diffraction (SAXRD) pattern of the as-prepared alumina in Fig. 3(a) indicates that as-prepared alumina possesses ordered mesoporous structure. The sample has a sharp diffraction peak and one weak peak at 2θ around 1.0° and 1.8°, respec-

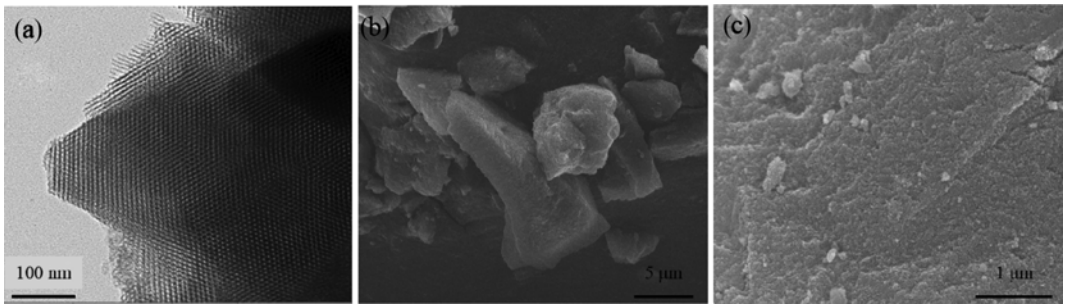

Fig. 1. TEM (a) and SEM (b), (c) images of mesoporous alumina.

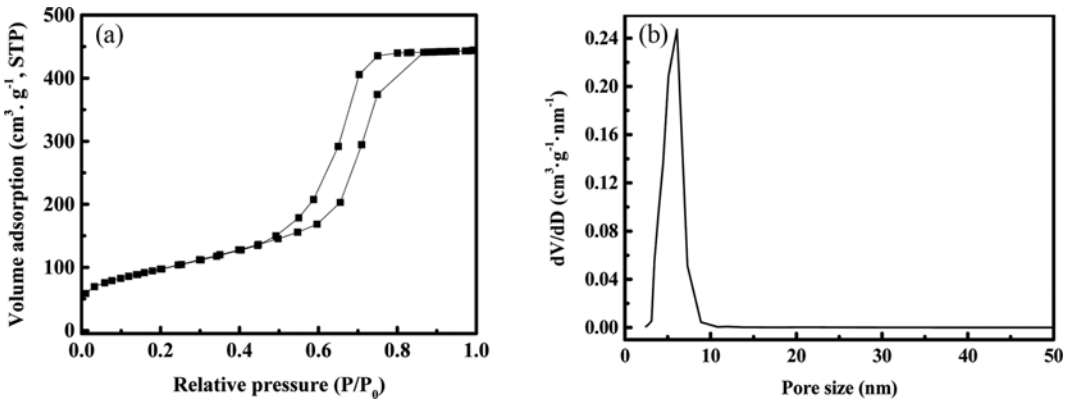

Fig. 2. N_2 adsorption-desorption isotherm (a) and pore size distribution (b) of mesoporous alumina.

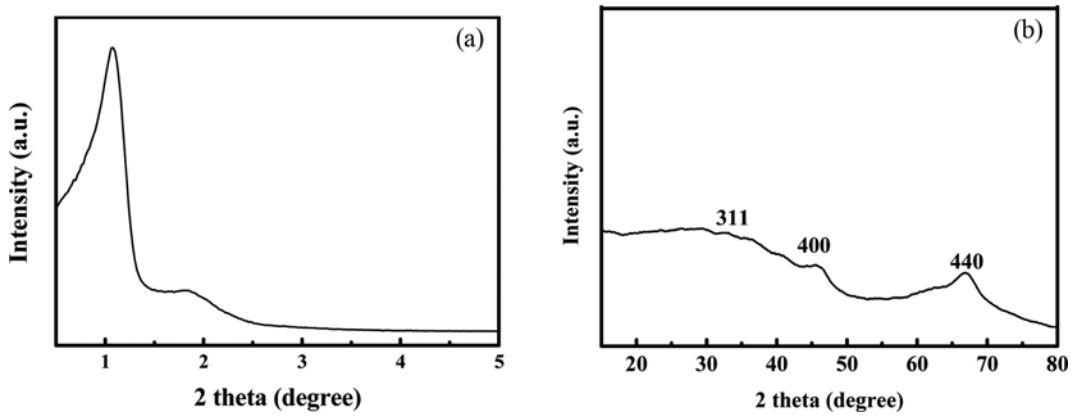

Fig. 3. SAXRD (a) and WAXRD (b) patterns of mesoporous alumina.

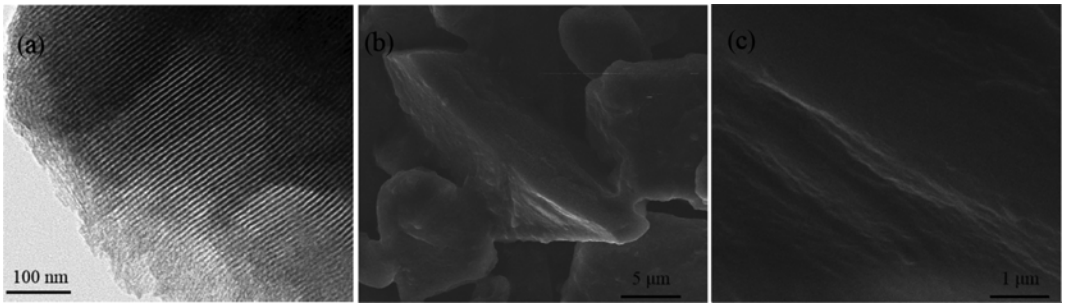

Fig. 4. TEM (a) and SEM (b), (c) images of IL-MA composite material.

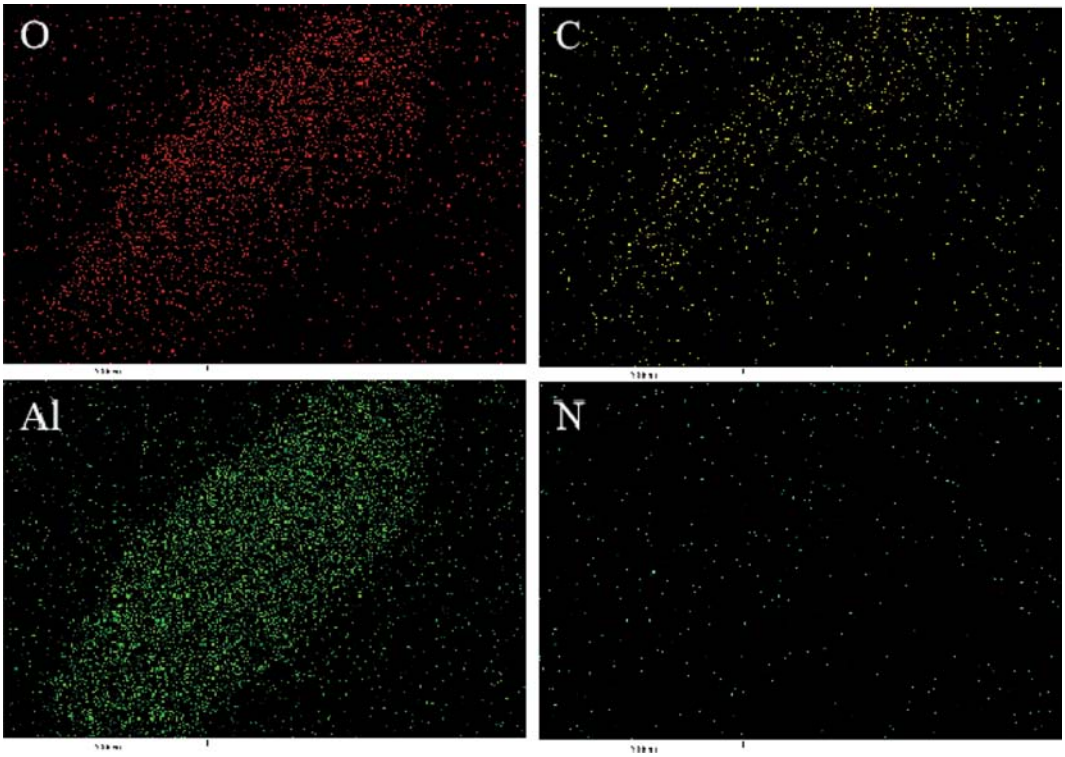

Fig. 5. Elemental mapping images of IL-MA composite material.

tively. This determination proves that alumina has a high degree of 2D hexagonal structure [25], which is consistent with the TEM image (Fig. 1(a)). Fig. 3(b) shows the wide-angle X-ray diffraction (WAXRD) pattern of the alumina calcined at 700 °C. There are

three diffraction peaks indexed to be the (440), (400) and (311) of γ-Al_2O_3 phase (JCPDS Card No. 29-0063), which demonstrates that γ-Al_2O_3 has been obtained at 700 °C.

2. Characterizations of IL-MA Composite Material

The morphology of bi-functionalized IL-MA composite material was also observed by TEM and SEM, as shown in Fig. 4. According to Fig. 4(a), the structure of the composite material keeps ordered mesostructure well. Pore structure and size of the composite material almost maintain unchanged after introducing ionic liquids compared with mesoporous alumina (Fig. 1(a)). SEM image also indicates that the morphology of the composite material keeps irregular. Compared with Fig. 1(c), the surface of IL-MA composite material (See Fig. 4(c)) is relatively smooth, which indicates that the outer surface is covered with IL. The mapping images (Fig. 5) confirm the presence of C, N elements, which further indicates that IL is present in the composite material. According to nitrogen adsorption-desorption isotherm, the specific surface area and the pore volume of the composite material are only about 0.03 m^2/g and nearly zero, respectively. This confirms that the pores of mesoporous alumina are occupied by ionic liquid in the composite material.

Thermogravimetric analyses were conducted to study and compare the thermal properties of bi-functionalized ionic liquid and IL-MA composite material. Fig. 6(a) shows TG and DTG curves of pure ionic liquid [MOEmim][Gly]. Owing to the high water-absorbing ability of amino acid ionic liquids [30], there is about 9.8% mass loss of [MOEmim][Gly] from 50 to 170 °C, which mainly is the removal of adsorbed water and small molecules. The loss of sample mass is 40% in the temperature range from 180 to 250 °C. This is attributed to the decomposition of glycinate ($[Gly]^-$). It can be seen from DTG curve in Fig. 6(a) that the mass loss gradually speeds up as the temperature further increases. This is because 1-methoxyethyl-3-methyl imidazolium group ($[MOEmim]^+$) starts to decompose. Above 350 °C, TG curve begins to be flat and the value of DTG curve is close to zero. These results reveal that the ionic liquid decomposed completely at 350 °C.

The mass loss of mesoporous alumina was also characterized: there is only about 3% mass loss from 40 to 100 °C. Since mesoporous alumina has been calcined at 700 °C for 4 h, the mass loss is the removal of adsorbed water from atmosphere in the process of loading sample. And the mass loss of IL-MA composite materials can be seen in Fig. 6(b). There is still about 6% mass loss from 40 to 150 °C, which also is the removal of adsorbed water and small molecules including acetone molecules. In view of the existence of moisture, the initial point m_1 in equation (1) is the sample mass at 150 °C. It can be observed that the initial decomposition temperature is 190 °C and the mass of IL-MA composite material continue to decrease from 190 °C to 600 °C. This should be attributed to the decomposition of [MOEmim][Gly]. The mass of the composite material remains constant above 600 °C. This indicates that ionic liquid in composite material decomposes completely. In comparison, the decomposition temperature range of IL-MA composite materials is much wider than that of pure IL, owing to the van der Waals' force between the bi-functionalized ionic liquid and mesoporous alumina. Ionic liquid loading capacity of IL-MA composite material can reach 1.04 g IL·g MA^{-1} in this experiment.

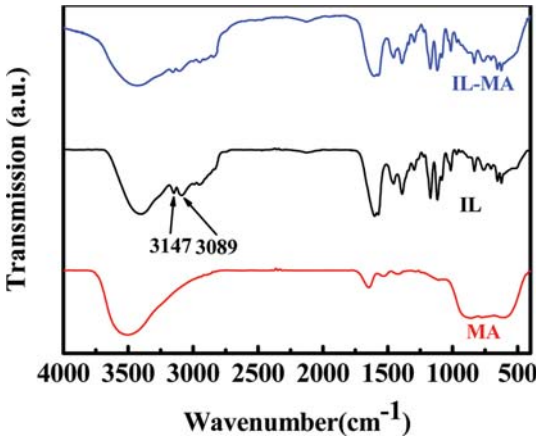

Fig. 7. FT-IR spectra of mesoporous alumina, bi-functionalized ionic liquid and IL-MA composite material.

3. FT-IR Analysis

The FT-IR spectroscopic analyses of mesoporous alumina, bi-functionalized ionic liquid and IL-MA composite material were studied, respectively. As shown in Fig. 7, the FTIR spectrum of IL-MA has the characteristics of bi-functionalized ionic liquid and mesoporous alumina. The peaks of 3,147 and 3,089 cm^{-1} in bi-functionalized ionic liquid are C-H stretching vibration bands of imidazole ring [31]. Based on the equivalent test samples, the peak intensity of C-H stretching vibration bands of imidazole ring for IL-

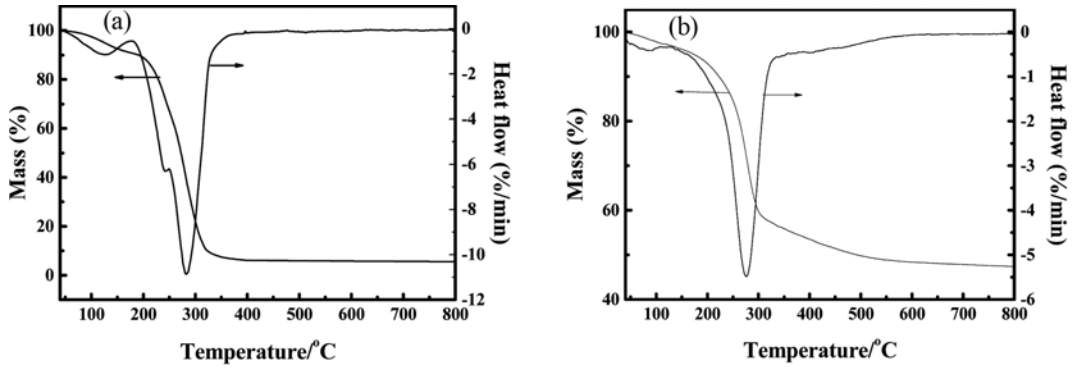

Fig. 6. TG and DTG curves of [MOEmim][Gly] (a) and IL-MA composite material (b).

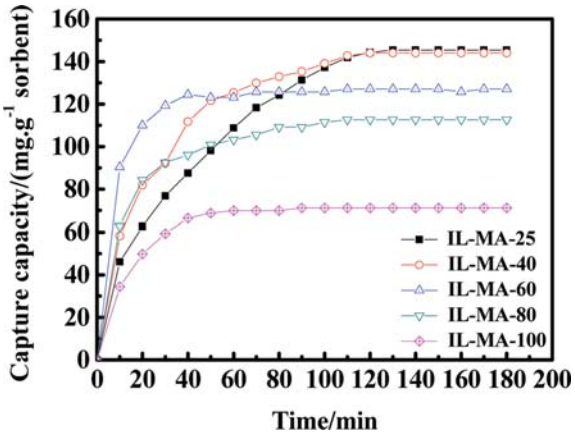

Fig. 8. CO_2 capture capacity of IL-MA composite material *vs* time at different temperatures.

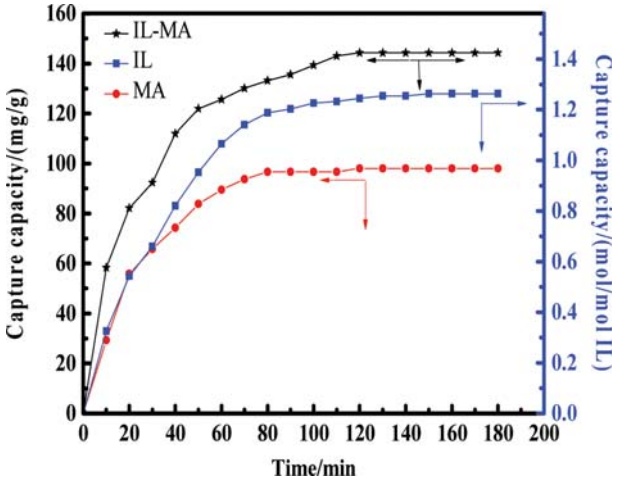

Fig. 9. CO_2 capture capacity of different sorbents *vs* time at 40 °C.

MA sample is a little weaker compared with IL. It should be ascribed to the formation of hydrogen bond between imidazole ring of ionic liquid and alumina in composite material, which can decrease the electron density of C-H band in imidazole ring [32]. FTIR spectroscopy analysis further confirms that bi-functionalized ionic liquid is successfully immobilized in mesoporous alumina through ultrasonic-assisted impregnation method.

4. Capture Capacity of IL-MA Composite Material

The effect of temperature on CO_2 capture by IL-MA composite material was studied at ambient pressure. As shown in Fig. 8, the capture capacity of IL-MA composite material is 145 and 144 mg CO_2·g sorbent^{-1} at the temperature of 25 and 40 °C, respectively. CO_2 capture ability constantly decreases as temperature further increases and the capacity is only 71 mg CO_2·g sorbent^{-1} at 100 °C. At the initial stage of the experiment, the CO_2 capture amount in the composite material increased linearly over time. The capture rate of composite material at 40 °C is higher than that at 25 °C and equilibrium is reached in about 70 and 120 min, respectively. But the fastest capture rate occurs at 60 °C, and this is attributed to the two competitive effects of temperature on gas capture. On one hand, high temperature can accelerate the gas mass transfer rate, which is beneficial to CO_2 capture. On the other hand, elevated temperature will weaken the bond of sorbent and gas, leading to the gas desorption. When the temperature increases to 60 °C, the gas mass transfer plays a dominant role in gas capture, so the capture rate is faster than that at 25 °C and 40 °C; With the further increase of capture temperature, the binding force between CO_2 molecules and sorbent becomes weaker and weaker while gas desorption gradually becomes stronger, resulting in the decrease of the capture rate. Based on both the capture capacity and capture rate, 40 °C is selected as the capture temperature in the following experiments.

To further understand CO_2 capture performance of IL-MA composite material, the capture capacities of [MOEmim][Gly] and mesoporous alumina were studied at 40 °C for comparison (see Fig. 9). For the IL-MA composite material, the pore channel and surface of mesoporous alumina are almost occupied by ionic liquid. In this case, ionic liquid supported by mesoporous alumina will play major role in CO_2 capture. As a result, the composite material possesses higher capture efficiency than IL alone and the capture capacity of IL-MA composite material (1.42 mol/mol IL) is apparently higher than that of pure [MOEmim][Gly] (1.26 mol/mol IL). The equilibrium time in composite material is about 110 min, which is shorter than that in IL (140 min). The possible reason is that: for pure ionic liquid [MOEmim][Gly], its viscosity is high (288.6 cP, 25 °C) and continuously increases during the absorption process. Obviously, it is difficult to achieve complete reaction between ionic liquid and CO_2 [11]; For IL-based composite material, ionic liquid can uniformly distribute on the surface and in the pore channel of the solid support, resulting in more complete contact and thus more sufficient chemical adsorption between carbon dioxide and the ionic liquid [MOEmim][Gly]. Moreover, mesoporous alumina as solid support can also physically adsorb CO_2; therefore, the combination of physical adsorption and chemical absorption for IL-MA composite can effectively enhance the CO_2 capture capacity. The slow growth and final equilibration of capture capacity of [MOEmim][Gly] after 80 min is attributed to its high viscosity. As shown in Fig. 9, the capture capacity of IL-MA composite material (144 mg·g^{-1}) is also higher than that of MA (98 mg·g^{-1}) based on the mass of adsorbents. The CO_2 capture rate of the composite material is faster than that of MA in initial stage due to the chemical reaction between ionic liquid and CO_2. But the equilibrium time in the composite material is longer than that in MA (80 min), which is because the channel of alumina narrows down after immobilizing ionic liquid and carbon dioxide needs more time to enter alumina channel.

The sorption capacities of different sorption materials were compared with our composite material and summarized in Table 1. From Table 1, the maximum sorption capacity of [MOEmim][Gly]/MA in our work is higher than mono-functionalized ionic liquid based composite materials [12,13,25], although it is lower than the vast majority of amine-functionalized solid composite materials [5, 24,33].

5. Reuse of IL-MA Composite Material

The result of Fig. 8 also demonstrates that low-temperature captured CO_2 can be desorbed at higher temperature. However, elevated temperature could lead to the decomposition of IL-MA

Table 1. Comparison of CO_2 sorption capacities using different sorption materials

Adsorbent	Maximum sorption capacity ($mg \cdot g^{-1}$)	Capture conditions	Reference
[MOEmim][Gly]/MA	144	40 °C, 1 bar	This work
PAP/Pa	52.8	20 °C, 1 bar	12
PAP/M41	81	20 °C, 1 bar	12
$[C_4PYP][Tf_2N]$/MCM-41	77	25 °C, 1 bar	13
[Emim][Gly]/MA	111	30 °C, 1 bar	25
Amine-DBU	132	25 °C, 1 bar	24
HP20/PEI-50	181	25 °C, 1 bar	5
3dd-TEPA60%	224	75 °C, 1 bar	33

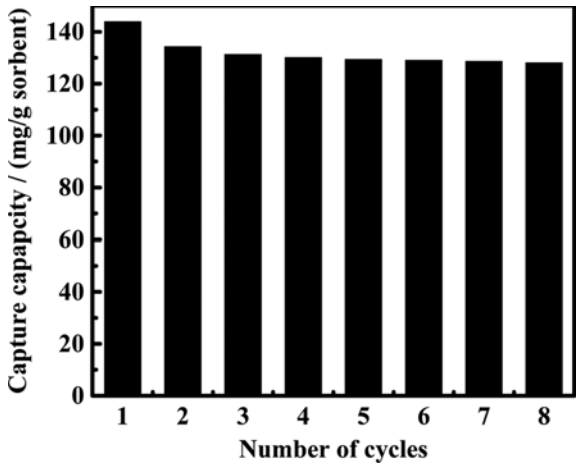

Fig. 10. Effect of recycle times on CO_2 capture capacity of IL-MA composite material.

composite materials (shown in Fig. 6(b)). Here, the saturated sorbent was heated at 150 °C to investigate the regeneration performance of IL-MA composite material. The effect of recycle times on CO_2 capture capacity of IL-MA composite material is shown in Fig. 10. Compared to the first cycle of capture-regeneration, the capture capacity of the second cycle slight decreases from 144 to 134 mg $CO_2 \cdot g\ sorbent^{-1}$. It is possible that a small amount of CO_2 molecules are deeply embedded into the pores of the composite material, leading to incomplete CO_2 desorption. According to Fig. 10, the composite material can be used for at least eight cycles without noticeable loss of efficiency. For comparison, the regeneration stability of pure [MOEmim][Gly] was studied in our previous work and the result showed that [MOEmim][Gly] could be used at least five cycles with stable absorption capacity [26]. As we expect, the combination of IL and MA can also improve the regeneration stability.

Specific surface area and pore volume of eight-cycled composite material are 0.07 m^2/g and 0.001 cm^3/g, respectively. The slight increase of specific surface area and pore volume indicates a little loss of ionic liquid after eight-cycle of CO_2 capture-regeneration, owing to the weak binding force of [MOEim][Gly] and mesoporous alumina in the composite material synthesized with impregnation method. Meanwhile, the loss of ionic liquid also leads to the decrease of CO_2 capture capacity.

CONCLUSIONS

Bi-functionalized IL-MA composite material was successfully synthesized for CO_2 capture. And the composite material maintained ordered mesostructure of alumina and had higher thermostability than [MOEmim][Gly]. The maximum capture capacity of IL-MA composite material reached 1.42 $mol \cdot mol\ IL^{-1}$ (144 mg $CO_2 \cdot g\ sorbent^{-1}$) at 40 °C, which is higher than that of [MOEmim][Gly] alone at the same temperature. CO_2 capture capacity of composite material kept well after recycling for eight times. Through this study, a new composite material with high CO_2 capture capacity was achieved *via* a facile route. To get closer to the real atmosphere, the research of CO_2 capture from simulate flue gas is ongoing.

ACKNOWLEDGEMENTS

This project was financially supported by the National Natural Science Foundation of China (21206118) and PetroChina Innovation Foundation (2013D-5006-0402).

REFERENCES

1. H. Fashandi, M. Zarrebini, A. Ghodsi and R. Saghafi, *J. Colloid Interface Sci.*, **476**, 35 (2016).
2. Z. Dai, R. D. Noble, D. L. Gin, X. Zhang and L. Deng, *J. Membr. Sci.*, **497**, 1 (2016).
3. Y. S. Sistla and A. Khanna, *Chem. Eng. J.*, **273**, 268 (2015).
4. W. Fan, Y. Liu and K. Wang, *J. Clean Prod.*, **125**, 296 (2016).
5. Z. Chen, S. Deng, H. Wei, B. Wang, J. Huang and G. Yu, *ACS Appl. Mater. Inter.*, **5**, 6937 (2013).
6. Y. Zhang, J. Sunarso, S. Liu and R. Wang, *Int. J. Greenh. Gas Con.*, **12**, 84 (2013).
7. H. K. Cho, J. E. Kim and J. S. Lim, *Korean J. Chem. Eng.*, **34**, 1475 (2017).
8. Y. Uehara, D. Karami and N. Mahinpey, *Ind. Eng. Chem. Res.*, **56**, 14316 (2017).
9. C. Wang, H. Luo, H. Li, X. Zhu, B. Yu and S. Dai, *Chem. Eur. J.*, **18**, 2153 (2012).
10. L. Y. Zhou, X. M. Shang, J. Fan and J. J. Wang, *J. Chem. Thermodyn.*, **103**, 292 (2016).

11. Y. Zhang, S. Zhang, X. Lu, Q. Zhou, W. Fan and X. Zhang, *Chem-Eur. J.*, **15**, 3003 (2009).
12. M. M. Wan, H. Y. Zhu, Y. Y. Li, J. Ma, S. Liu and J. H. Zhu, *ACS Appl. Mater. Inter.*, **6**, 12947 (2014).
13. K. Kumar and A. Kumar, *J. Phys. Chem. C*, **122**, 8216 (2018).
14. J. Zhu, F. Xin, J. Huang, X. Dong and H. Liu, *Chem. Eng. J.*, **246**, 79 (2014).
15. F. Nkinahamira, T. Su, Y. Xie, G. Ma, H. Wang and J. Li, *Chem. Eng. J.*, **326**, 831 (2017).
16. A. Erto, A. Silvestre-Albero, J. Silvestre-Albero, F. Rodriguez-Reinoso, M. Balsamo, A. Lancia and F. Montagnaro, *J. Colloid Interface Sci.*, **448**, 41 (2015).
17. L. Xu, H. Zhao, H. Song and L. Chou, *Int. J. Hydrogen Energy*, **37**, 7497 (2012).
18. M. Tian, Y. Long, D. Xu, S. Wei and Z. Dong, *J. Colloid Interface Sci.*, **521**, 132 (2018).
19. M. G. Plaza, C. Pevida, B. Arias, J. Fermoso, A. Arenillas, F. Rubiera and J. J. Pis, *J. Them. Ana. Calorim.*, **92**, 601 (2008).
20. Y. Lara and L. M. Romeo, *Energy Procedia*, **114**, 2380 (2017).
21. B. Ekka, R. S. Dhaka, R. K. Patel and P. Dash, *J. Clean Prod.*, **151**, 303 (2017).
22. C. Gunathilake, M. Gangoda and M. Jaroniec, *Ind. Eng. Chem. Res.*, **55**, 5598 (2016).
23. H. Jeon, S. H. Ahn, J. H. Kim, Y. J. Min and K. B. Lee, *J. Mater. Sci.*, **46**, 4020 (2011).
24. C. E. S. Fuentes, D. Guzman-Lucero, M. Torres-Rodriguez, N. V. Likhanova, J. N. Bolanos, O. Olivares-Xometl and I. V. Lijanova, *Sep. Purif. Technol.*, **182**, 59 (2017).
25. M. Balsamo, A. Erto, A. Lancia, G. Totarella, F. Montagnaro and R. Turco, *Fuel*, **218**, 155 (2018).
26. L. Sun, J. Luo and S. Tang, *Chem. J. Chinese U.*, **38**, 1578 (2017).
27. W. Qian, Y. Xu, B. Xie, Y. Ge and H. Shu, *Int. J. Greenh. Gas. Con.*, **56**, 194 (2017).
28. Q. Yuan, A. X. Yin, C. Luo, L. D. Sun, Y. W. Zhang, W. T. Duan, H. C. Liu and C. Hua, *J. Am. Chem. Soc.*, **130**, 3465 (2008).
29. S. Tang, X. Cui, L. Gu, H. Zhou and X. Zhang, *Funct. Mater. Lett.*, **6**, e1350059 (2013).
30. E. D. Bate, R. D. Mayton, I. Nta and J. H. Davis, *J. Am. Chem. Soc.*, **124**, 926 (2002).
31. A. Ahmed, Y. Chaker, E. H. Belarbi, O. Abbas, J. N. Chotard, H. B. Abassi, N. V. Nhien, M. E. Hadri and S. Bresson, *J. Mol. Struct.*, **1173**, 653 (2018).
32. W. H. Yu, H. Zhang, Z. P. Lei, H. F. Shui, S. G. Kang, Z. C. Wang, S. B. Ren and C. X. Pan, *Fuel*, **236**, 861 (2019).
33. G. J. Zhang, P. Y. Zhao, Y. Xu, Z. X. Yang, H. Z. Cheng and Y. F. Zhang, *ACS Appl. Mater. Inter.*, **10**, 34340 (2018).